# Design of Thick-Lamination Rotor Configuration for a High-Speed Induction Machine in Megawatt Class

Tuhin Choudhury, Juuso Narsakka, Iikka Martikainen, Eerik Sikanen, Emil Kurvinen, Rafal P. Jastrzebski, *Member, IEEE* Juha Pyrhönen, *Senior Member, IEEE* and Jussi Sopanen, *Member, IEEE*

***Abstract*—Solid rotors are preferred choice of topology for high-speed applications due to their robustness against high centrifugal forces at high speeds, ease of manufacturability, and higher temperature range. However, for peripheral speeds lower than 200 m/s, laminated rotor structure is preferred because of lower eddy current losses resulting in higher efficiency. However, laminated rotors are complex to manufacture, sensitive to temperature and have vibration and mechanical integrity related issues. As a compromise between these two designs in terms of mechanical strength and efficiency, this study investigates a radial flux 2 MW, 15 krpm induction motor rotor core made of thick laminations. The baseline dimensions of the thick-lamination rotor design are calculated using analytical equations considering aspects such as mechanical stresses, rotordynamics, and bearing parameters. Lastly, the lamination to lamination contact behavior under unbalance load is analyzed for a simplified model and their effect on natural frequencies is studied.**

***Index Terms*—Thick-lamination rotor, High-Speed, Megawatt class, Induction machine, Rotordynamics, Stress analysis**

## I. Introduction

High-speed (HS) electrical machines are used in a wide range of applications in modern industry [1] because of their high-power density and smaller footprint compared to conventional machines [2]. In applications such as compressors, the possibility of high-speed range of operation eliminates the requirement for geared systems and for a mechanical coupler, leading to direct drives, and integrated solution with low maintenance [3]. The most popular types of HS machines are the induction machines (IMs) and permanent magnet synchronous machines (PMSMs). However, the HS IM is mostly preferred because of its simple and rigid construction, ease of manufacturability, and relatively low-cost material requirements [1].

While there is no exact criterion that classifies a machine as a high-speed one, the classification is often based on the speed of the rotor relative to its size. For example, most researchers consider a rotor spinning with peripheral velocities above 100-150 m/s as a HS machine, as described by Jokinen and Luomi [4] as well as Binder and Schneider [5].

In high-speed electric machines the rotor can be made in several configurations. Two of the most popular categories are the solid rotors and laminated rotors.

Majority of the HS IMs are designed using either laminated or solid rotor construction. A laminated rotor is typically chosen for speeds below 200 m/s and they can achieve significantly (2-3 %) higher efficiency, mostly due to lower rotor eddy current losses [6]. However, designing such rotors for higher speeds becomes challenging due to mechanical and thermal limitations. In some cases, as demonstrated by Lateb et al. [7], special topology can be used where a laminated rotor core, with embedded copper bars, copper end plates, and end shafts fixed by tie rods was reported to achieve peripheral speeds higher than 200 m/s.

In the laminated rotor standard electric machine laminates are used, i.e. which have insulation on both sides, that mitigates eddy current losses. The challenge comes when the rotor lamination stack has to be machined after the stack assembly possibly leading to short circuits between the laminates.

In addition, assembling of the rotor requires additional considerations to achieve a straight and rigid package. In order to achieve this, end rings are used to maintain the robustness and for example, shrink fits are used to mount the laminates to the rotor shaft. The machining of the rotor lamination stack after the stack assembly is also challenging due the possibility of short circuiting the laminates.

For machines with very high surface velocity, the solid rotor becomes the only option that can handle excessive loads. Typically, laminated rotors become challenging over 200 m/s surface velocities, and maximum speed that physically can be achieved are in the range of 350-400 m/s [8]. The main benefits of a solid rotor include ease of manufacturing and robustness, as it is made from a single piece of steel, which is then machined to dimensions and grooves or squirrel cage is then arranged. The drawback of a solid rotor is its poor electromagnetic performance, which leads to higher rotor losses and therefore high rotor temperatures, easily above 150 °C [9]. This can, however,

T. Choudhury (corresponding author), J. Narsakka, I. Martikainen, E. Sikanen, and Prof. J. Sopanen are with Department of Mechanical Engineering, Lappeenranta-Lahti University of Technology LUT, Yliopistonkatu 34, 53850 Lappeenranta, Finland, Tuhin.Choudhury@lut.fi

Prof. E. Kurvinen is with Materials and Mechanical Engineering University of Oulu, Pentti Kaiteran katu 1, 90570 Oulu, Finland

R. P. Jastrzebski, and J. Pyrhönen are with Department of Electrical Engineering, Lappeenranta-Lahti University of Technology LUT, Yliopistonkatu 34, 53850 Lappeenranta, Finland.

be strongly mitigated by sophisticated stator design.

As something that is in between these two extremes, a thick-lamination rotor topology can be proposed that combines the benefits of a solid rotor and a laminated rotor design. The basic principle is that the laminated sheet metals are replaced with thick steel plates. High strength steel with good electromagnetic features [10] can be used and insulation between rotor laminates can be manually done to reduce rotor stack eddy current losses. For example, sheet metal manufacturing techniques, e.g. laser cutting, can be applied easily with 10 mm thick steel plates and have good surface quality.

Therefore, the objective of the study is to design a 2 MW thick-laminate rotor for an induction motor and analyze the stress and rotordynamic performance of such a machine. The design has a squirrel cage arrangement with copper end rings. Analytical equations are utilized to determine the important baseline dimensions of the rotor and the mechanical stresses in the system. Lastly, the laminate to laminate contact is analyzed using 3-D Finite Element Method (FEM), and the effect of the contacts on the natural frequencies under different magnitude of radial unbalance loads are investigated.

## II. Method

### A. Baseline dimensions

*1) Active part dimensions:* Although the dimensions of the rotor are mainly limited by the stresses and mechanical limits of material, the active part of the rotor is usually calculated based on electromagnetic aspects derived from the required power and speed. A common approach is to use mechanical machine constant at the conceptual stage to calculate the roughly suitable length and diameter [11]:

$$C_{\text{mec}} = \frac{P_{\text{mec}}}{D^2 \cdot l \cdot n_{\text{syn}}}, \tag{1}$$

where $C_{\text{mec}}$ is the machine constant, $P_{\text{mec}}$ is the power, $D$, $l$ and $n_{\text{syn}}$ are the diameter, effective length and synchronous speed of the active part. The value of machine constant can be obtained from literature [12] for a given value of power and number of pole pairs ($p$). Typically, HS machines use 2-pole configuration for lower motor losses [13]. Therefore, for totally enclosed asynchronous machines, the length to diameter ratio, $\chi$, can be calculated according to [12] as:

$$\chi = \frac{l}{D} = \frac{\pi}{2p}\sqrt[3]{p}. \tag{2}$$

Once the effective length and outer diameter of the active part are figured out, the next step is to identify the diameter of the solid core of the rotor and the thickness, inner and outer diameter of the laminates. These dimensions are mainly driven by the stresses due to velocity and temperature. A larger diameter of the solid core ensures the mechanical stiffness required for the rigidity of the rotor at high speeds. Similarly the thickness of the laminates contributes to the stiffness of the stack. The stiffness of the rotor increases with increasing disk thickness. Therefore, the optimum thickness is rather dependent on the manufacturability and assembly procedure to ensure minimum gap between the laminates. However, below a certain level of laminate thickness, the additional stiffness with laminate configuration can be presumed to be insignificant compared to thin-laminate stacks. With the squirrel cage configuration ensuring proper electromagnetic conductivity, high strength alloys with relatively low electrical conductivity than S355 can be considered for the laminates.

In case of solid rotor core with thick laminates and squirrel cage, the usable cross section for the laminates and end ring of squirrel cage are critical factors. The laminate type structure with load due to rotational velocity is a studied topic in interior permanent magnet (IPM) machines [14]. It can be implemented also with a thick laminate rotor design with certain restrictions. The micro gaps between the laminates act as radial slots, consequently enhancing the cooling of the electric machine. Therefore, the temperature effects such as creeping can be left out from baseline design. While FE-analysis are suitable for detailed design, for baseline design at conceptual stage, analytical equations can be used for identifying the stresses in the laminates due to centrifugal forces [15]. The radial and tangential stresses on the rotating laminates due to centrifugal forces can be given as:

$$\sigma_r = \frac{3+\nu_d}{8}\rho_{\text{d}}\Omega^2(r_{\text{in}}^2 + r_{\text{out}}^2 - \frac{r_{\text{in}}^2 r_{\text{out}}^2}{r_{\text{y}}^2} - r_{\text{y}}^2), \tag{3}$$

$$\sigma_\theta = \frac{3+\nu_{\text{d}}}{8}\rho_d\Omega^2(r_{\text{in}}^2 + r_{\text{out}}^2 + \frac{r_{\text{in}}^2 r_{\text{out}}^2}{r_{\text{y}}^2} - \frac{1+3\nu_{\text{d}}}{3+\nu_{\text{d}}}r_{\text{y}}^2), \tag{4}$$

where $\nu_{\text{d}}$ is the Poisson's ratio, $\rho_{\text{d}}$ is the density of the laminate, $r_{\text{in}}$ is the laminate inner radius and $r_{\text{out}}$ outer radius [16]. Eqs. (3) and (4) can be used to calculate the stresses using solid rotor radius ($r_s$) as well as for the laminates with their inner radius as $r_s$ and outer radius as $r_{do}$. Note that in detailed design, inner radius of the laminate will differ from the radius of the solid core depending on the details of shrink fit such as interference, tolerances, and coefficient of thermal expansion of the individual materials. However, for the baseline design at the conceptual stage, only nominal dimensions are considered.

Furthermore, additional stress concentration in the laminates can occur depending on the bar shape and rotor slot opening width ($b$) and height ($h$) (Fig.1). A study by Barta et al. [11] on squirrel cage rotor design showed that even a narrow slot opening can significantly improve the machine performance. However, to account for the slot opening in analytical calculations, the identified stresses from Eqs. (3) and (4) have to be multiplied by a stress concentration factor ($k_{\text{slot}}$). $k_{\text{slot}}$ which can be obtained from previous studies and charts on stresses due to notches [17], or from FEM.

For the squirrel cage design, the bars and the end rings are the conducting components, which make them

very significant from the electromagnetic perspective. The materials of the end rings should have similar conductivity as that of the bar [12]. Although high level of conductivity is preferable, the material should be strong enough to withstand large centrifugal forces acting especially on the end rings. Typically, high strength copper alloys such as CuCrZr, Cu-Be, and $CuAl_2O_3$ are used for such HS applications [6]. To reinforce the end rings, additional support sleeves (outer radius $r_{so}$ in Fig. 1) made of high strength, non magnetic material are often employed [11].

For ease of assembly, the rotor shaft can feature a collar on one end and the laminates have to be loaded from the other end of the rotor, enclosed by a threaded lock disk or an end plate at the very end. The copper rings are mounted on the shaft collar on one end, and an extended flange of the lock disk at the other (outer radius $r_{\text{epo}}$ in Fig. 1). The mechanical stresses for the laminates and sleeves can be calculated similarly as the rotor laminates from Eqs. (3),(4), multiplied by stress concentration factor for ring of holes in circular thin element [17].

*2) Bearings:* The bearing selection largely depends on the application itself and the external load. However, for HS applications, generally active magnetic bearings (AMBs) are preferred because of their numerous advantages [18]. The general dimensioning of the rotor shaft for radial and axial AMBs at the conceptual design stage has been discussed in details in [15]. The radius of the shaft in the AMB section is roughly determined relative to the active part of the rotor. Next, the specific load capacity based on achievable magnetic pressure (typically 30 - 40 N/cm$^2$) and dynamic load factor over 4 is used used to determine the length of the AMBs [19]. Radials AMBs are usually separated from the sensors using a spacer to avoid electromagnetic interference between the sensor and the radial actuator. Suitable angular

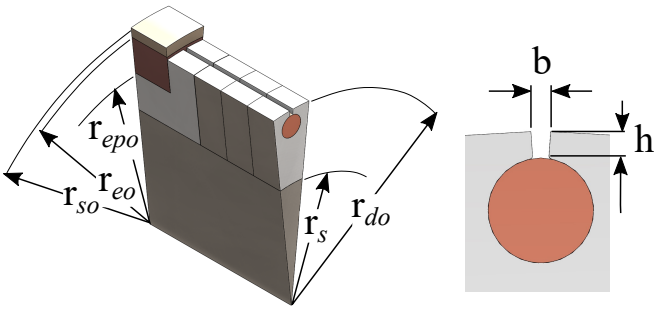


Fig. 1. Key nominal dimensions for calculating the stresses in the active part of a thick laminate rotor

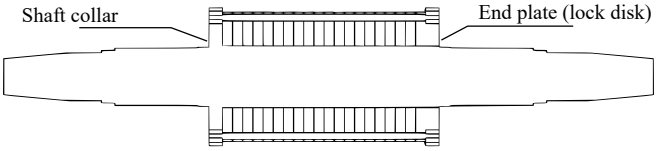


Fig. 2. Thick-laminate rotor cross section with a shaft collar on one end and a lock disk or end plate on the other.

contact ball bearings (two for each end) based on the rotor load, speed and end shaft dimensions can be used as backup bearing [15].

### B. Thick-laminate to laminate contact analysis

Proper contact treatment between thick laminates in the thick-laminate rotor concept becomes important as the rotor can bend under certain amount of unbalance force. The operational deflection shape can change the contact status between laminates, thus, changing the rotor natural frequencies. Proper contact modeling can be challenging, as the shrink fitted laminates obviously are not bonded together, but they also do not experience rigid body displacements or rotations. On the other hand, they can elastically deform under suitable loads such as centrifugal and unbalance-induced speed-dependent loads. The most suitable contact type for numerical analysis is frictional contact type between two adjacent laminates. Either frictional sliding forces are included of not, the contact can be open or closed, depending on the current loading conditions [20]. Thus, either frictional, or numerically simpler frictionless non-linear contact is required to achieve most realistic behavior. In such a case of shrink fitted laminates, the laminates are heated to a higher temperature, which often can yield micro gaps between the laminates as the temperature difference evens out. Hydraulic preload can be applied during the cooling down process to press the laminates together, but often, due to increasing frictional forces between laminates and the shaft as the temperatures get closer to environment temperature, minor gaps can be expected.

At no-load, the laminate stack will have different natural frequencies compared to the situation when a large enough force, such as unbalance force at high speed operating, is present. Excluding the coriolis effect, the change in the contact status causes two separate effects that will shift the natural frequencies of the system at non-zero speeds. First, the changed contact status will often stiffen the system. In thick-laminate rotor case, the effect can be particularly strong for the first forward whirling mode. Second, under tensile stress state, the system can experience additional stress stiffening effect, which will stiffen the system when pre-stress state is included into eigenvalue analysis [21].

## III. Results and Discussions

### A. Baseline design of a 2 MW rotor

Based on the equations and justifications mentioned in Section II-A, a baseline model is designed in the study for a 2 MW application operating at 15 krpm. Fig. 3 shows the rotor geometry designed in CAD using the dimensions from the analytical calculations. Table I highlights the main nominal dimensions of the rotor and Fig. 4 shows the stresses from the components of the active part of the rotor.

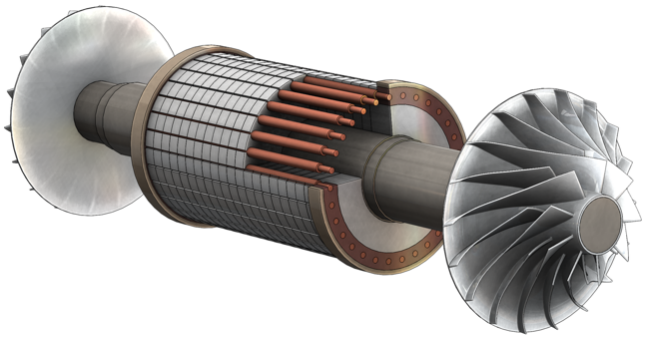

Fig. 3. Thick-laminate rotor cross section with a shaft collar on one end and a lock disk or end plate on the other.

TABLE I
THICK-LAMINATE ROTOR MAIN PARAMETERS AND DIMENSIONS

| Parameters | Case study |
|---|---|
| **Active part** | |
| Active part length (mm) | 454.68 |
| Solid core diameter (mm) | 180.00 |
| Laminate outer diameter (mm) | 290.00 |
| Laminate thickness (mm) | 20.00 |
| Tangential stress (EM) (kPa) | 21.28 |
| Core stress (max) (MPa) | 64.33 |
| Laminate stress (max) (MPa) | 362.00 |
| Surface velocity (m/s) | 227.34 |
| **End ring and Sleeve** | |
| End Ring inner diameter (mm) | 238.00 |
| End Ring outer diameter (mm) | 294.00 |
| Sleeve outer diameter (mm) | 309.00 |
| End ring and sleeve thickness (mm) | 30.00 |
| **Section 1 after active part** | |
| S1 shaft Diameter (mm) | 174.46 |
| S1 shaft length (each side) (mm) | 25.00 |
| **Ends of Rotor** | |
| End shaft diameter (mm) | 109.00 |
| End shaft length (each side) (mm) | 225.00 |
| **Section 2 after AMB** | |
| S1 shaft diameter (mm) | 159.46 |
| S1 shaft length (each side) (mm) | 30.00 |
| **AMB dimensions** | |
| Radial AMB inner diameter (mm) | 169.46 |
| Radial AMB outer diameter (mm) | 209.46 |
| Radial AMB sleeve length (mm) | AMB 1: 117.45, AMB 2: 105.79 |
| Axial AMB diameter (mm) | 109.00 |
| Axial AMB outer diameter (mm) | 290.00 |
| Axial AMB sleeve length (mm) | 20.00 |
| Spacer inner diameter (mm) | 169.46 |
| Spacer outer diameter (mm) | 199.46 |
| Spacer length (mm) | 20.00 |
| Total mass of rotor (kg) | 493.96 |

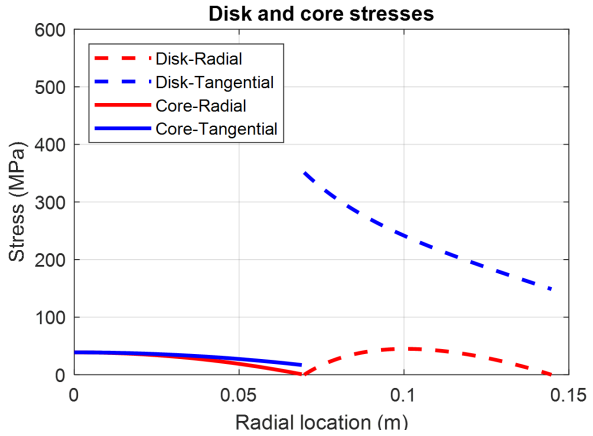


(a)

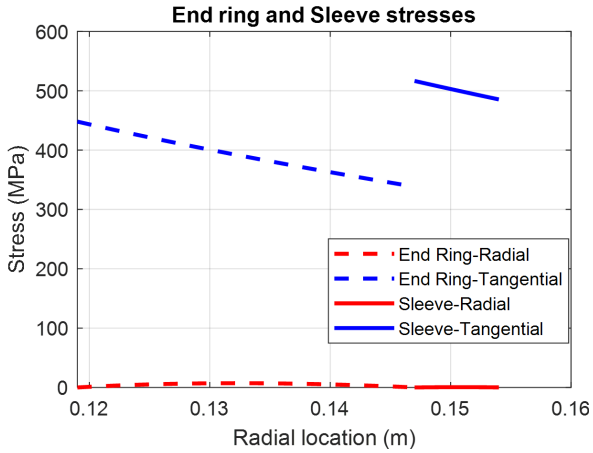


(b)

Fig. 4. Stresses in (a) disk and rotor core and (b) end ring and sleeve w.r.t radial location ($r_y$).

### *B. Contact cases with varied unbalance loads and effect on frequency*

*1) Simplified test case with four thick laminates:* For contact analysis, a simplified model is considered. Fig. 5 shows the model consisting of a thin long shaft (50 mm diameter, 300 mm long) with four thick laminates (250 mm diameter and 10 mm thickness) mounted on it. The laminates have a micro-gap of 10 $\mu$m between them.

With the simplified thin shaft case, the effect of the stiffness of the shaft is reduced so that the behavior of the laminate to laminate contact can be isolated and analyzed under different load conditions. Fig. 6 shows the contact profile in between the laminates for different values of unbalance at different speeds.

For the damped frequency analysis, two of the unbalance cases are compared with the no load case. The change in damped frequencies of the first bending mode pair are obtained using 3D FEM modeling in ANSYS software (Fig. 7). There is a small relative offset (approximately 1 Hz) in the frequencies for the large unbalance case starting at the zero speed which continues throughout the speed range. This is probably due to the large mass of the attached unbalance

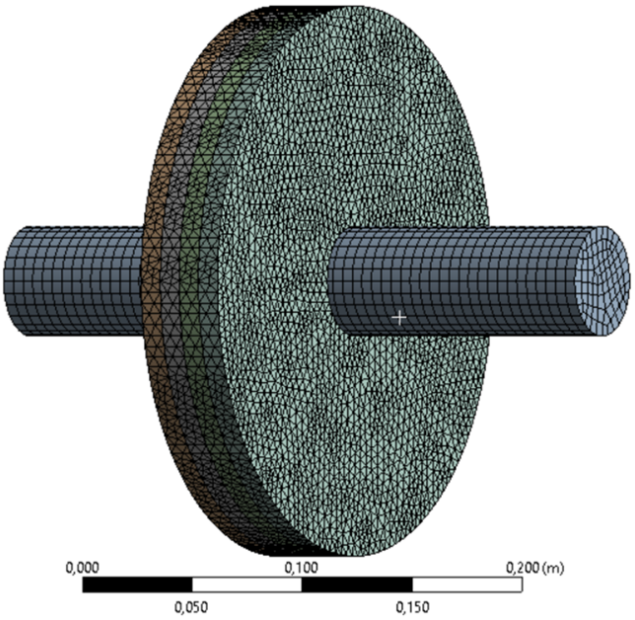


Fig. 5. Simple four laminate rotor with a thin shaft mounted on bearings at both ends. Unbalance masses are added at the outer radius of the laminates.

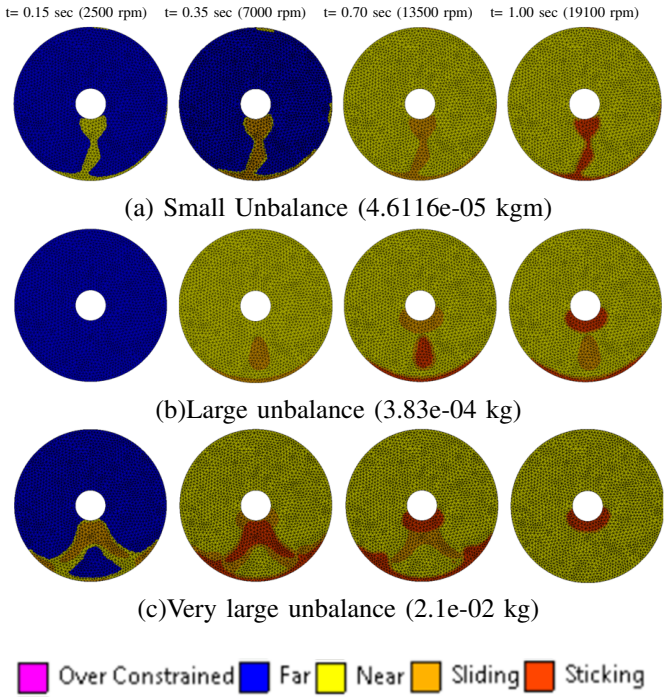


Fig. 6. Contact profile variation for three different unbalance cases for the four thick laminates rotor case for a 1 second long simulation with rotational speed ramped from 0 to 19100 rpm.

(21 g) relative to the rotor mass (20 kg).

*2) Baseline rotor:* For the rotor designed using the baseline analytical equations, the unbalanced masses were attached at 270 degrees. Fig. 8 shows that the laminates close to the centre of the active part have the highest contact. With this setup, three different cases of permissible unbalance

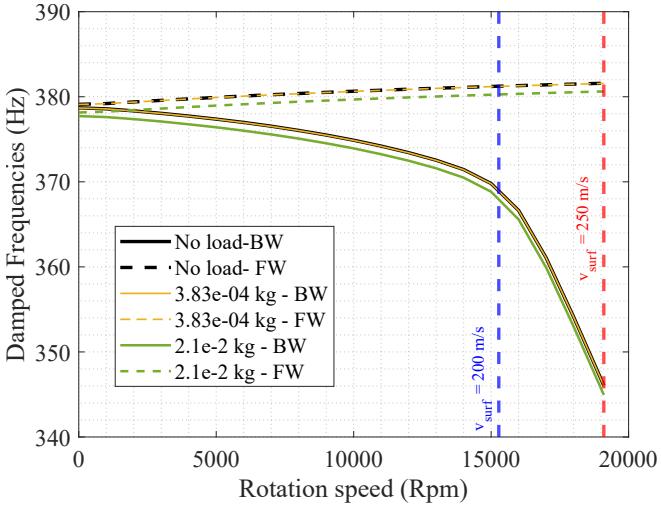


Fig. 7. The calculated changes in the natural frequencies of the simple two thick laminate rotor under different unbalance load

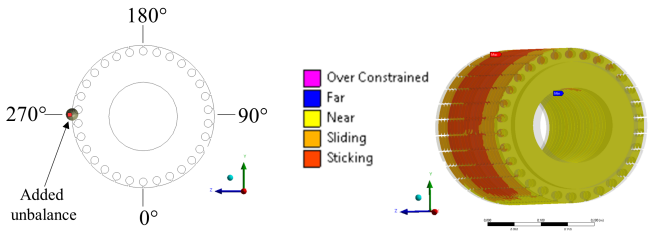


Fig. 8. (a) Unbalance location for contact analysis in baseline rotor for 2 MW thick-laminate rotor. (b) Contact profile of the array of laminates under the radial load.

corresponding to balancing grades G 1.0, G 2.5 and G 6.3 were tested. Fig. 9 shows the contact profile for the baseline rotor.

## IV. Discussion

Part of the paper focuses on the design of the thick lamination rotor using analytical equations for high power induction motor applications. Since only the mechanical aspects are considered in the analytical stress calculation, a factor of safety of 1.5 can be included. With that in

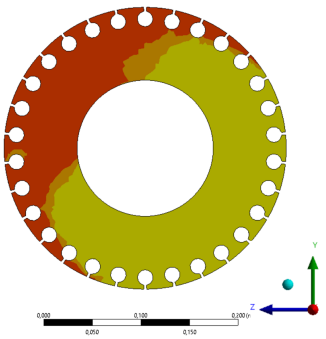

Fig. 9. Contact profile of the cross section of the unbalanced laminate with its adjacent laminates for three different cases from G1.0 to G 6.3

mind, the stresses of the laminates, end ring, and sleeves can be approximated as 525 MPa, 675 MPa and 765 MPa, respectively. For the laminate material, 42CrMo4 can be considered as a good choice. At its current dimension, the end ring presents more challenges in terms of balance between strength of the copper alloy, and its electrical conductivity. For example, while CuZr, CuCr or CuCrZr have best electrical conductivity at room temperature (80-93 % IACS), their yield strength is insufficient for this case [13]. However, with a sleeve, which can be made of carbon fibre composite, the stresses on the end ring can be mitigated which could potentially make the highly conductive material usable. Alternatively, CuBe can be used for the end ring to withstand the current stresses [13].

Following the stress analysis, the contact behavior of the thick laminations are further analyzed. With increase in load and speed, there is a general trend of increase in contact area and magnitude. However, for the same load the contact profile varies extensively with speed. For example, in case Fig. 6(c) with very high unbalance, the contact region at 19100 rpm is rather small compared to the lower unbalance cases. Similarly, for Fig. 6(a) at 2500 rpm, the contact between the laminates is already initiated, which is not the same for case (b) with higher load at the same speed. Therefore, the results show that the contact region and duration are not entirely dependent on the unbalance mass but more on the speed. This could be because the unbalance force is dependent on the square of the speed and therefore with higher forces, the closed contact areas remain pressed together for longer duration.

In the damped frequency analysis, for all the cases, the forward mode shows steady increase in frequency, which can be attributed to the gyroscopic forces. However, at high speeds, the backward whirling frequencies start decreasing rapidly for all the cases. Approximately above 200 m/s surface velocity, the backward whirling frequencies for the different cases start to coincide. This shows that irrespective of the unbalance load, the effect due to the contact stiffnesses dominates the behavior at high speeds.

Lastly for the contact analysis of the baseline rotor model, the profile in Fig. 9 shows close sticking behavior in the region of the applied load. The contact profile remains the same for all cases of unbalance because the contacts are not changing extensively in this case compared to the simplified model because of relatively thicker core shaft.

## V. Conclusions

The objective of the study was to design a thick-laminate rotor with squirrel configuration as an intermediate topology between a solid rotor and a laminated rotor for an induction motor. The study utilized analytical methods to identify the key nominal dimensions of the rotor from mechanical and rotordynamic point of view. The stresses on the thick laminates, end rings and sleeves could be used to choose the appropriate material for those parts at conceptual stage. The baseline model can be considered as an initial starting point for further interdisciplinary investigation such as thermal and electromagnetic analysis before the final design. Furthermore, the contact analysis shows that the frequencies of such rotors are affected by the pre-stress due to radial load such as unbalance. The opening and closing of non-linear frictional contact affects the stiffnesses. The amount of contact between laminates and the contact region is largely dependent on the speed of the motor. At higher speeds, stiffness asymmetry occurs which further increases the gap between the bending mode frequencies. For a balanced rotor, such effects can be mitigated by increasing the rotor core diameter. However, the contact stiffnesses are automatically updated in ANSYS which influences the result based on the number of nodes in contact. Therefore, for a more concrete understanding, a thorough contact analysis with variable stiffness is required in the future.

## References


[1] N. Uzhegov, *Design and material selection of high-speed rotating electrical machines*. Ph.D. dissertation, Dept. Elec. Eng., Lappeenranta University of Technology, 2016.

[2] N. Bianchi, S. Bolognani, and F. Luise, "Potentials and limits of high-speed pm motors," *IEEE Transactions on Industry Applications*, vol. 40, no. 6, pp. 1570–1578, 2004.

[3] J. Huppunen, *High-speed solid-rotor induction machine–electromagnetic calculation and design*. Ph.D. dissertation, Dept. Mech. Eng., Lappeenranta University of Technology, 2004.

[4] T. Jokinen and J. Luomi, "High-speed electrical machines," in *Conference on high speed technology, Lappeenranta, Finland*, 1988, pp. 175–185.

[5] A. Binder and T. Schneider, "High-speed inverter-fed ac drives," in *2007 International Aegean Conference on Electrical Machines and Power Electronics*. IEEE, 2007, pp. 9–16.

[6] D. Gerada, A. Mebarki, N. L. Brown, K. J. Bradley, and C. Gerada, "Design aspects of high-speed high-power-density laminated-rotor induction machines," *IEEE Transactions on Industrial Electronics*, vol. 58, no. 9, pp. 4039–4047, 2010.

[7] R. Lateb, J. Enon, and L. Durantay, "High speed, high power electrical induction motor technologies for integrated compressors," in *2009 International Conference on Electrical Machines and Systems*. IEEE, 2009, pp. 1–5.

[8] D. Gerada, A. Mebarki, N. L. Brown, C. Gerada, A. Cavagnino, and A. Boglietti, "High-speed electrical machines: Technologies, trends, and developments," *IEEE transactions on industrial electronics*, vol. 61, no. 6, pp. 2946–2959, 2013.

[9] J. Lähteenmäki, *Design and voltage supply of high-speed induction machines*. Ph.D. dissertation, Dept. Elec. Eng., Helsinki University of Technology, 2002.

[10] P. Lindh, P. Immonen, C. Di, M. Degano, and J. Pyrhönen, "Solid-rotor material selection for squirrel-cage high-speed solid-rotor induction machine," in *IECON 2019 - 45th Annual Conference of the IEEE Industrial Electronics Society*, vol. 1, 2019, pp. 1357–1361.

[11] J. Barta, N. Uzhegov, P. Losak, C. Ondrusek, M. Mach, and J. Pyrhönen, "Squirrel-cage rotor design and manufacturing for high-speed applications," *IEEE Transactions on Industrial Electronics*, vol. 66, no. 9, pp. 6768–6778, 2018.

[12] J. Pyrhönen, T. Jokinen, and V. Hrabovcova, *Design of rotating electrical machines*. John Wiley & Sons, 2013.

[13] F. Zhang, Y. Li, and G. Du, "Comparative study on structure of laminated-rotor high-speed induction machine," in *2014 17th International Conference on Electrical Machines and Systems (ICEMS)*. IEEE, 2014, pp. 3175–3179.

[14] P. Arumugam, Z. Xu, A. La Rocca, G. Vakil, M. Dickinson, E. Amankwah, T. Hamiti, S. Bozhko, C. Gerada, and S. J. Pickering, "High-speed solid rotor permanent magnet machines: Concept and design," *IEEE Transactions on Transportation Electrification*, vol. 2, no. 3, pp. 391–400, 2016.

[15] E. Kurvinen, T. Choudhury, J. Narsakka, I. Martikainen, J. Sopanen, and R. P. Jastrzebski, "Design space method for conceptual design exploration of high speed slitted solid induction motor," in *2021 IEEE International Electric Machines & Drives Conference (IEMDC)*. IEEE, 2021, pp. 1–8.
[16] A. Borisavljevic, *Limits, modeling and design of high-speed permanent magnet machines*. Springer, 2012.
[17] W. D. Pilkey, D. F. Pilkey, and Z. Bi, *Peterson's stress concentration factors*. John Wiley & Sons, 2020.
[18] E. H. Maslen and G. Schweitzer, *Magnetic bearings: theory, design, and application to rotating machinery*. Springer, 2009.
[19] R. P. Jastrzebski, A. Putkonen, E. Kurvinen, and O. Pyrhönen, "Design and modeling of 2 mw amb rotor with three radial bearing-sensor planes," *IEEE Transactions on Industry Applications*, vol. 57, no. 6, pp. 6892–6902, 2021.
[20] M. A. Puso and T. A. Laursen, "A Mortar Segment-to-Segment Frictional Contact Method for Large Deformations," *Computer Methods in Applied Mechanics and Engineering*, vol. 193, pp. 4891–4913, 2004.
[21] K. S. S. Aradhya and Y. L. Narayana, "Study of Stress-Stiffening Effect on the Dynamic Response of Fan-Disc Assembly of a Fighter Aircraft Engine," *56th Congress of Indian Society of Theoretical and Applied Mechanics*, vol. 56, 2011.

## VI. Biographies

**Tuhin Choudhury** was born in Seppa, India, in 1989. He received the B.Sc. (tech) degree in mechanical engineering from Sikkim Manipal University, India, in 2011, and the M.Sc. degree in mechatronic system design from LUT University, Lappeenranta, Finland, in 2018, where he is currently pursuing the Ph.D. degree with the Department of Mechanical Engineering. He was a design engineer on the development of medical devices and diagnostic instruments, from 2011 to 2016. His research interests include designing, modeling, and simulation of rotating machines, and the analysis of rotor behavior to understand the root cause of unwanted vibrations, specifically due to unbalance.

**Juuso Narsakka** was born in Rautjärvi, Finland, in 1989. He received B. Sc. (Tech.) degrees in mechanical engineering from Lappeenranta University of Technology (LUT) in 2020, where he is currently pursuing the M. Sc. degree in mechatronic system design. His research interests are in the design of high-speed rotating machines where is needed combination of an understanding of machine dynamics and strength of materials. His work history includes jobs in industry, entrepreneurship, and teaching in LUT University.

**Iikka Martikainen** received the M.Sc. degree in mechanical engineering from Lappeenranta University of technology (LUT) in 2020 and is currently pursuing the D.Sc. (Technology) degree at Laboratory of Machine dynamics, LUT. His research interest include high-speed rotor dynamics, focusing on three dimensional solid finite element and rolling bearing modelling.

**Eerik Sikanen** received the M.Sc. degree in mechanical engineering and the D.Sc. (technology) degree from LUT University, Lappeenranta, Finland, in 2014 and 2018, respectively. He is currently working as a Postdoctoral Researcher with the Laboratory of Machine Dynamics, LUT. His research interests are high-speed rotor dynamics analysis and general vibration dynamics of rotating machinery. He is mainly concentrating on three-dimensional solid finite element modeling of high-speed machinery and systems including contact and thermomechanical effects.

**Emil Kurvinen** was born in 1988. He received M. Sc. (Tech.) and D. Sc. (Tech.) degrees in mechanical engineering from Lappeenranta University of Technology (LUT) in 2012 and 2016, respectively. In 2014-2015 he visited University of Virginia as a Fulbright visiting scholar researching active magnetic bearings. In 2016 to 2017 he served as a engineer, structural dynamics in FS Dynamics Finland Ltd. In 2017-2021 he was as a postdoctoral researcher at LUT. Currently he is Machine Design professor in University of Oulu. He has a solid background in machine design, especially in the design, simulation, analysing of rotating machines. His research interests are rotating machines, especially high-speed machines, digital twins and integration of industrial engineering and management to technology.

**Rafal Piotr Jastrzebski** (Member, IEEE) received the M.Sc. degree in electrical engineering from the Technical University of Lodz, Poland, in 2002, and the D.Sc. degree in electrical engineering from the Lappeenranta University of Technology (LUT), Finland, in 2007. At LUT, he is currently an Adjunct Professor. His research interests include design, modeling, and control of electric machines, sensors, and power electronics. He has long experience in digital control, system engineering of energy applications, mechatronic systems, active magnetic bearings, magnetic levitation systems, and bearingless machines. From 2013 to 2018, he was an Academy Research Fellow. From 2009 to 2011, he was a recipient and served as an Academy of Finland Postdoctoral Researcher.

**Juha J. Pyrhönen** (M'06, SM'17) born in 1957 in Kuusankoski, Finland, received the Doctor of Science (D.Sc.) degree from Lappeenranta University of Technology (LUT), Finland in 1991. He became Professor of Electrical Machines and Drives in 1997 at LUT. He is engaged in research and development of electric motors and power-electronic-controlled drives. Prof. Pyrhönen has wide experience in the research and development of special electric drives for e.g. distributed power production, traction and high-speed applications. Permanent magnet materials and applying them in machines have an important role in his research. Currently he is also studying possibilities of using carbon-based materials in electrical machines.

**Jussi Sopanen** (Member, IEEE) was born in Enonkoski, Finland, in 1974. He received the M.Sc. degree in mechanical engineering and the D.Sc. (technology) degree from LUT University, Lappeenranta, Finland, in 1999 and 2004, respectively. He was a Researcher with the Department of Mechanical Engineering, LUT University, from 1999 to 2006. He was a Product Development Engineer of electric machine manufacturing with Rotatek Finland Ltd. from 2004 to 2005. From 2006 to 2012, he was a Principal Lecturer in mechanical engineering and the Research Manager of the Faculty of Technology, Saimaa University of Applied Sciences, Lappeenranta. He is currently serving as a Professor with the Machine Dynamics Laboratory, LUT University. His research interests include rotor dynamics, multibody dynamics, and the mechanical design of electrical machines.